

# Lagrangian method for multiple correlations in passive scalar advection

U. Frisch<sup>1</sup>, A. Mazzino<sup>1,2</sup>, A. Noullez<sup>1</sup> and M. Vergassola<sup>1</sup>

<sup>1</sup> CNRS, Observatoire de la Côte d'Azur, B.P. 4229, 06304 Nice Cedex 4, France.

<sup>2</sup> INFN–Dipartimento di Fisica, Università di Genova, I–16146 Genova, Italy.

(February 9, 2018)

A Lagrangian method is introduced for calculating simultaneous  $n$ -point correlations of a passive scalar advected by a random velocity field, with random forcing and finite molecular diffusivity  $\kappa$ . The method, which is here presented in detail, is particularly well suited for studying the  $\kappa \rightarrow 0$  limit when the velocity field is not smooth. Efficient Monte Carlo simulations based on this method are applied to the Kraichnan model of passive scalar and lead to accurate determinations of the anomalous intermittency corrections in the fourth-order structure function as a function of the scaling exponent  $\xi$  of the velocity field in two and three dimensions. Anomalous corrections are found to vanish in the limits  $\xi \rightarrow 0$  and  $\xi \rightarrow 2$ , as predicted by perturbation theory.

PACS number(s): 47.10.+g, 47.27.-i, 05.40.+j

## I. INTRODUCTION

Robert Kraichnan's model of passive scalar advection by a white-in-time velocity field has been particularly fertile ground for theoreticians trying to develop a theory of intermittency [1–3] (see also Refs. [4,5]). Although the model leads to closed equations for multiple-point moments, only second-order moments can be obtained in closed analytic form [6]. Theoretical predictions differed as to the behavior of higher-order quantities, regarding in particular the survival or the vanishing of intermittency corrections (anomalies) in certain limits. Obtaining reliable numerical results was thus an important challenge. Until recently numerical simulations have been based on the direct integration of the passive scalar partial differential equation and have been limited to two dimensions [5,7,8]. Such calculations are delicate; to wit, the difficulty of observing for the second-order structure function the known high-Péclet number asymptotic scaling [6]. Also, the numerical scheme used in Refs. [5,7] involves a slightly anisotropic velocity field which is not expected to give exactly the right scaling laws for the passive scalar [9].

Lagrangian methods for tackling the Kraichnan model and which require only the integration of ordinary differential equations were recently proposed independently by Frisch, Mazzino and Vergassola [10] and by Gat, Procaccia and Zeitak [11]. Our goal here is to give a detailed presentation of the Lagrangian method and to present new results.

In Section II we give the theoretical background of the Lagrangian method for general random velocity fields which need not be white-in-time. In Section III we investigate the limit of vanishing molecular diffusivity which depends crucially on how nearby Lagrangian trajectories separate. We then turn to the Kraichnan model which is given a Lagrangian formulation (Section IV). Then, we show how it can be solved numerically by a Monte-Carlo method (Section V) and present results in both two and three space dimensions (Section VI). We make concluding remarks in Section VII.

## II. THE LAGRANGIAN METHOD

The (Eulerian) dynamics of a passive scalar field  $\theta(\mathbf{r}, t)$  advected by a velocity field  $\mathbf{v}(\mathbf{r}, t)$  is described by the following partial differential equation (written in space dimension  $d$ ):

$$\partial_t \theta(\mathbf{r}, t) + \mathbf{v}(\mathbf{r}, t) \cdot \nabla \theta(\mathbf{r}, t) = \kappa \nabla^2 \theta(\mathbf{r}, t) + f(\mathbf{r}, t), \quad (1)$$

where  $f(\mathbf{r}, t)$  is an external source (forcing) of scalar and  $\kappa$  is the molecular diffusivity. In all that follows we shall assume that  $\theta(\mathbf{r}, t) = 0$  at some distant time in the past  $t = -T$  (eventually, we shall let  $T \rightarrow \infty$ ).

In this section the advecting velocity  $\mathbf{v}$  and the forcing  $f$  can be either deterministic or random. In the latter case, no particular assumption is made regarding their statistical properties.

In order to illustrate the basic idea of the Lagrangian strategy, let us first set  $\kappa = 0$ . We may then integrate (1) along its characteristics, the Lagrangian trajectories of tracer particles, to obtain

$$\theta(\mathbf{r}, t) = \int_{-T}^t f(\mathbf{a}(s; \mathbf{r}, t), s) ds, \quad (2)$$

where  $\mathbf{a}(s; \mathbf{r}, t)$  is the position at time  $s \leq t$  of the fluid particle which will be at position  $\mathbf{r}$  at time  $t$ . (Two-time Lagrangian positions of this type were also used in Kraichnan's Lagrangian History Direct Interaction theory [12].) This Lagrangian position, which will henceforth be denoted just  $\mathbf{a}(s)$ , satisfies the ordinary differential equation

$$\frac{d\mathbf{a}(s)}{ds} = \mathbf{v}(\mathbf{a}(s), s), \quad \mathbf{a}(t) = \mathbf{r}. \quad (3)$$

For  $\kappa > 0$  we shall now give a stochastic generalization of this Lagrangian representation. Roughly,  $\theta$  will be the average of a random field  $\phi$  which satisfies an advection–forcing equation with no diffusion term, in which the advecting velocity is the sum of  $\mathbf{v}$  and a suitable white-noise velocity generating Brownian diffusion.

To be more specific we need to introduce some notation. We shall use a set of  $n$   $d$ -dimensional time-dependent random vectors

$$\dot{\mathbf{w}}_i(s) = \{\dot{w}_{i,\alpha}; i = 1, \dots, n; \alpha = 1, \dots, d\}, \quad (4)$$

which are Gaussian, identically distributed, independent of each other and independent of both  $\mathbf{v}$  and  $f$ . The time dependence is assumed to be white noise:

$$\langle \dot{w}_{i,\alpha}(s) \dot{w}_{j,\beta}(s') \rangle_w = \delta_{ij} \delta_{\alpha\beta} \delta(s - s'). \quad (5)$$

The notation  $\langle \cdot \rangle_w$  stands for ‘‘average over the  $\dot{\mathbf{w}}_i$ ’s for a fixed realization of  $\mathbf{v}$  and  $f$ ’’. Similarly,  $\langle \cdot \rangle_{vf}$  stands for ‘‘average over  $\mathbf{v}$  and  $f$  for a fixed realization of the  $\dot{\mathbf{w}}_i$ ’s’’. Unconditional averages are denoted just  $\langle \cdot \rangle$ . Clearly,

$$\langle \cdot \rangle = \langle \langle \cdot \rangle_w \rangle_{vf} = \langle \langle \cdot \rangle_{vf} \rangle_w. \quad (6)$$

The white noise, which is a random distribution, is here denoted by  $\dot{w}(s)$  since it is the time derivative of the Brownian motion (or Wiener–Lévy) process. In the numerical implementation we shall work with increments of  $w(s)$ .

We can now state the main result which is at the basis of our Lagrangian method.

Let  $\phi_i(\mathbf{r}, t)$  ( $i = 1, \dots, n$ ) be the solutions of the following advection–forcing equations:

$$\begin{aligned} \partial_t \phi_i(\mathbf{r}, t) + \left( \mathbf{v}(\mathbf{r}, t) + \sqrt{2\kappa} \dot{\mathbf{w}}_i(t) \right) \cdot \nabla \phi_i(\mathbf{r}, t) &= f(\mathbf{r}, t). \\ \phi_i(\mathbf{r}, -T) &= 0, \quad i = 1, 2, \dots, n. \end{aligned} \quad (7)$$

For any  $\mathbf{r}_1, \mathbf{r}_2, \mathbf{r}_3, \dots$ , we have

$$\theta(\mathbf{r}_1) = \langle \phi(\mathbf{r}_1) \rangle_w, \quad \forall i \quad (8)$$

$$\theta(\mathbf{r}_1) \theta(\mathbf{r}_2) = \langle \phi_i(\mathbf{r}_1) \phi_j(\mathbf{r}_2) \rangle_w, \quad \forall i \neq j, \quad (9)$$

$$\begin{aligned} \theta(\mathbf{r}_1) \theta(\mathbf{r}_2) \theta(\mathbf{r}_3) &= \langle \phi_i(\mathbf{r}_1) \phi_j(\mathbf{r}_2) \phi_k(\mathbf{r}_3) \rangle_w, \\ \forall i, j, k, \quad i \neq j \neq k \neq i, \end{aligned} \quad (10)$$

.....

where all the fields  $\theta$  and  $\phi$  are evaluated at the same time  $t$ .

The proof of (8) is obtained by taking the mean value of (7) (only over  $w$ ) and noting that

$$\left\langle \sqrt{2\kappa} \dot{\mathbf{w}}_i \cdot \nabla \phi_i \right\rangle_w = -\kappa \nabla^2 \langle \phi_i \rangle_w. \quad (11)$$

(This is a standard result for linear stochastic equations having white-noise coefficients; it is derived using Gaussian integration by parts (see Ref. [13], Chap. 4). For similar derivations see Refs. [6,14,15].)

To prove (9), we first derive from (7), assuming  $i \neq j$ ,

$$\begin{aligned} \partial_t (\phi_i(\mathbf{r}_1) \phi_j(\mathbf{r}_2)) + [\mathbf{v}(\mathbf{r}_1) \cdot \nabla_1 + \mathbf{v}(\mathbf{r}_2) \cdot \nabla_2 \\ + \sqrt{2\kappa} (\dot{\mathbf{w}}_i \cdot \nabla_1 + \dot{\mathbf{w}}_j \cdot \nabla_2)] \phi_i(\mathbf{r}_1) \phi_j(\mathbf{r}_2) = \\ f(\mathbf{r}_1) \phi_j(\mathbf{r}_2) + f(\mathbf{r}_2) \phi_i(\mathbf{r}_1), \end{aligned} \quad (12)$$

where  $\nabla_1$  and  $\nabla_2$  stand for  $\nabla_{\mathbf{r}_1}$  and  $\nabla_{\mathbf{r}_2}$ . We then average (12) (over  $w$ ) and use a relation similar to (11)

$$\begin{aligned} \left\langle \sqrt{2\kappa} (\dot{\mathbf{w}}_i \cdot \nabla_1 + \dot{\mathbf{w}}_j \cdot \nabla_2) \phi_i(\mathbf{r}_1) \phi_j(\mathbf{r}_2) \right\rangle_w \\ = -\kappa (\nabla_1^2 + \nabla_2^2) \langle \phi_i(\mathbf{r}_1) \phi_j(\mathbf{r}_2) \rangle_w. \end{aligned} \quad (13)$$

(Notice that cross terms involving  $\nabla_1 \cdot \nabla_2$  disappear because of the independence of  $\dot{\mathbf{w}}_i$  and  $\dot{\mathbf{w}}_j$ .) The higher order equations in (10) and following are proved similarly.

Because of the absence of a diffusion operator in (7), its solution has an obvious Lagrangian representation

$$\phi_i(\mathbf{r}, t) = \int_{-T}^t f(\mathbf{a}_i(s), s) ds, \quad (14)$$

where

$$\frac{d\mathbf{a}_i(s)}{ds} = \mathbf{v}(\mathbf{a}_i(s), s) + \sqrt{2\kappa} \dot{\mathbf{w}}_i(s), \quad (15)$$

$$\mathbf{a}_i(t) = \mathbf{r}. \quad (16)$$

So far we have not used the random or deterministic character of  $\mathbf{v}$  and  $f$ . In the random case, taking the average of (8)–(10) over  $\mathbf{v}$  and  $f$ , we obtain

$$\langle \theta(\mathbf{r}_1) \rangle = \langle \phi(\mathbf{r}_1) \rangle, \quad \forall i \quad (17)$$

$$\langle \theta(\mathbf{r}_1) \theta(\mathbf{r}_2) \rangle = \langle \phi_i(\mathbf{r}_1) \phi_j(\mathbf{r}_2) \rangle, \quad \forall i \neq j \quad (18)$$

$$\begin{aligned} \langle \theta(\mathbf{r}_1) \theta(\mathbf{r}_2) \theta(\mathbf{r}_3) \rangle &= \langle \phi_i(\mathbf{r}_1) \phi_j(\mathbf{r}_2) \phi_k(\mathbf{r}_3) \rangle, \\ \forall i, j, k, \quad i \neq j \neq k \neq i, \end{aligned} \quad (19)$$

.....

Eqs. (14), (15), (16), together with (17), (18) and higher orders, constitute our Lagrangian representation for multiple-point moments of the passive scalar.

Let us stress that, for moments beyond the first order, it is essential to use more than one white noise. Indeed, we could have made use of just (8) and written

$$\theta(\mathbf{r}_1) \theta(\mathbf{r}_2) = \langle \phi_i(\mathbf{r}_1) \rangle_w \langle \phi_j(\mathbf{r}_2) \rangle_w, \quad \forall i, j. \quad (20)$$

(Including the case  $i = j$ .) It is however not possible to  $(\mathbf{v}, f)$ -average (20) because it involves a *product* of  $w$ -averages rather than just one average as in (9).

In the more restricted context of the Kraichnan model, a functional integral representation of  $n$ th order moments involving, as here,  $n$  white noises has already been given in Refs. [16,17].

### III. THE LIMIT OF VANISHING MOLECULAR DIFFUSIVITY

Interesting pathologies occur when we bring two or more Eulerian space arguments of the moments to coincidence and *simultaneously* let  $\kappa \rightarrow 0$ .

This is already seen on the second-order moment  $\langle \theta^2(\mathbf{r}_1) \rangle$ . From (14) and (18), we have

$$\langle \theta^2(\mathbf{r}_1) \rangle = \int_{-T}^t \int_{-T}^t \langle f(\mathbf{a}_i(s), s) f(\mathbf{a}_j(s'), s') \rangle ds ds', \quad (21)$$

for any  $i \neq j$ . The differential equations for  $\mathbf{a}_i(s)$  and  $\mathbf{a}_j(s)$  involve different white noises. If, in the limit  $\kappa \rightarrow 0$ , we simply ignore the  $\sqrt{2\kappa}\dot{\mathbf{w}}_i$  terms in (15), we find that all the  $\mathbf{a}_i(s)$ 's satisfy the same equation (3) and the same boundary condition  $\mathbf{a}_i(t) = \mathbf{r}_1$ . It is then tempting to conclude that all the  $\mathbf{a}_i(s)$ 's are identical, namely are just the Lagrangian trajectories  $\mathbf{a}(s)$  of the unperturbed  $\mathbf{v}$ -flow. As a consequence, we can then rewrite (21) as

$$\begin{aligned} \langle \theta^2(\mathbf{r}_1) \rangle &= \int_{-T}^t \int_{-T}^t \langle f(\mathbf{a}(s), s) f(\mathbf{a}(s'), s') \rangle ds ds', \\ &= \left\langle \left( \int_{-T}^t f(\mathbf{a}(s), s) ds \right)^2 \right\rangle. \end{aligned} \quad (22)$$

For a large class of random forcings  $f$  of zero mean the r.h.s. of (22) will diverge  $\propto T$  as  $T \rightarrow \infty$ . This is for example the case when  $f$  is homogeneous, stationary and short- (or delta-) correlated in time as in the Kraichnan model. The reason of this divergence is that, although the forcing has zero mean, its integral (along the Lagrangian trajectory) over times long compared to the correlation time behaves like Brownian motion (in the  $T$ -variable) and, thus, has a variance  $\propto T$ . From this naïve procedure we would thus conclude that, when  $T = \infty$ , the scalar variance becomes infinite as  $\kappa \rightarrow 0$ .

This conclusion is actually correct when the  $\mathbf{v}$ -flow is smooth (differentiable in the space variable): this is the so-called Batchelor limit which has been frequently investigated [6,16,18–21]. The conclusion however becomes incorrect when the  $\mathbf{v}$ -flow is only Hölder continuous, i.e. its spatial increments over a small distance  $\ell$  vary as a fractional power of  $\ell$  (e.g.  $\ell^{1/3}$  in Kolmogorov 1941 turbulence). As pointed out in Ref. [16] (see also Ref. [4]), when  $\mathbf{v}$  is not smooth the solution to (3) lacks uniqueness, so that two Lagrangian particles which end up at the same point  $\mathbf{r}_1$  at time  $t$  may have different past histories. This is exemplified with the one-dimensional model

$$\frac{dx}{ds} = -x^{1/3}, \quad -T \leq s \leq t, \quad x(t) = \epsilon \geq 0, \quad (23)$$

where  $x$  is a deputy for  $\mathbf{a}_i - \mathbf{a}_j$ , the separation between two nearby Lagrangian particles. For  $\epsilon > 0$ , the solution of (23) is

$$x(s) = \left[ \epsilon^{2/3} + \frac{2}{3}(t-s) \right]^{3/2}. \quad (24)$$

If we now set  $\epsilon = 0$  in (24) or consider times  $s$  such that  $|t-s| \gg \epsilon^{2/3}$ , we obtain

$$x(s) = \left[ \frac{2}{3}(t-s) \right]^{3/2}. \quad (25)$$

This is indeed a solution of (23) with  $\epsilon = 0$ , but there is another trivial one, namely  $x(s) = 0$ . Related to this non-uniqueness is the fact that, when  $\epsilon$  is small the solution given by (24) becomes independent of  $\epsilon$ , namely is given by the non-trivial solution (25) for  $\epsilon = 0$ .

Whenever the flow  $\mathbf{v}$  is just Hölder continuous, the separation of nearby Lagrangian particles proceeds in a similar way, becoming rapidly independent of the initial separation. Such a law of separation is much more explosive than would have been obtained for a smooth flow with sensitive dependence of the Lagrangian trajectories. In the latter case we would have  $x(s) = \epsilon e^{\lambda(t-s)}$  ( $\lambda > 0$ ), which grows exponentially with  $t-s$  but still tends to zero with  $\epsilon$ .

We propose to call this explosive growth a Richardson walk, after Lewis Fry Richardson who was the first to experimentally observe this rapid separation in turbulent flow and who was also much interested in the role of non-differentiability in turbulence [22]. It is this explosive separation which prevents the divergence of  $\langle \theta^2(\mathbf{r}_1) \rangle$  when  $\kappa \rightarrow 0$  (and more generally of moments with several coinciding points). Indeed, as the time  $s$  moves back from  $s = t$ , even an infinitesimal amount of molecular diffusion will slightly separate, say, by an amount  $\epsilon$ , the Lagrangian particles  $\mathbf{a}_i(s)$  and  $\mathbf{a}_j(s)$  which coincide at  $s = t$ . Then, the Richardson walk will quickly bring the separations to values independent of  $\epsilon$  and, thus of  $\kappa$ . Hence, the double integral in (21), which involves points  $\mathbf{a}_1(s)$  and  $\mathbf{a}_2(s)$  with uncorrelated forces when  $|s-s'|$  is sufficiently large, may converge for  $T \rightarrow \infty$ . (For it to actually converge more specific assumptions must be made about the space and time correlations of  $\mathbf{v}$  and  $f$ , which are satisfied, e.g., in the Kraichnan model.)

An alternative to introducing a small diffusivity is to work at  $\kappa = 0$ , with “point splitting”. For this one replaces  $\langle \theta^2(\mathbf{r}_1) \rangle$  by  $\langle \theta(\mathbf{r}_1) \theta(\mathbf{r}'_1) \rangle$ , where  $\mathbf{r}_1$  and  $\mathbf{r}'_1$  are separated by a distance  $\epsilon$ . Eventually,  $\epsilon \rightarrow 0$ . In practical numerical implementations we found that point splitting works well for second-order moments but is far less efficient than using a small diffusivity for higher-order moments.

#### IV. THE KRAICHNAN MODEL

The Kraichnan model [6,1] is an instance of the passive scalar equation (1) in which the velocity and the forcing are Gaussian white noises in their time dependence. This ensures that the solution is a Markov process in the time variable and that closed moment equations, sometimes called “Hopf equations”, can be written for single-time multiple-space moments such as  $\langle \theta(\mathbf{r}_1, t) \dots \theta(\mathbf{r}_n, t) \rangle$ . The equation for second-order moments was published for the first time by Kraichnan [6] and, for higher-order moments, by Shraiman and Siggia [20]. Note that Hopf’s work [23] dealt with the characteristic functional of random flow; it had no white-noise

process and no closed equations, making the use of his name not so appropriate in the context of white-noise linear stochastic equations. The fact that closed moment equations exist for such problems has been known for a long time (see, e.g., Ref. [14] and references therein). We shall not need the moment equations and shall not write them here (for an elementary derivation, see Ref. [15]).

The precise formulation of the Kraichnan model as used here is the following. The velocity field  $\mathbf{v} = \{v_\alpha, \alpha = 1, \dots, d\}$  appearing in (1) is incompressible, isotropic, Gaussian, white-noise in time; it has homogeneous increments with power-law spatial correlations and a scaling exponent  $\xi$  in the range  $0 < \xi < 2$ :

$$\langle [v_\alpha(\mathbf{r}, t) - v_\alpha(\mathbf{0}, 0)][v_\beta(\mathbf{r}, t) - v_\beta(\mathbf{0}, 0)] \rangle = 2\delta(t)D_{\alpha\beta}(\mathbf{r}), \quad (26)$$

where,

$$D_{\alpha\beta}(\mathbf{r}) = r^\xi \left[ (\xi + d - 1) \delta_{\alpha\beta} - \xi \frac{r_\alpha r_\beta}{r^2} \right]. \quad (27)$$

Note that since no infrared cutoff is assumed on the velocity its integral scale is infinite; this is not a problem since only velocity increments matter for the dynamics of the passive scalar. Note also that when a white-in-time velocity is used in (15), the well known Ito–Stratonovich ambiguity could appear [24]. This ambiguity is however absent in our particular case, on account of incompressibility.

The random forcing  $f$  is independent of  $\mathbf{v}$ , of zero mean, isotropic, Gaussian, white-noise in time and homogeneous. Its covariance is given by:

$$\langle f(\mathbf{r}, t) f(\mathbf{0}, 0) \rangle = F(r/L) \delta(t), \quad (28)$$

with  $F(0) > 0$  and  $F(r/L)$  decreasing rapidly for  $r \gg L$ , where  $L$  is the (forcing) integral scale.

In principle, to be a correlation, the function  $F(r/L)$  should be of positive type, i.e. have a non-negative  $d$ -dimensional Fourier transform. In our numerical work we find it convenient to work with the step function  $\Theta_L(r)$  which is equal to unity for  $0 \leq r \leq L$  and to zero otherwise. Hence, the injection rate of passive scalar variance is  $\varepsilon = F(0)/2 = 1/2$ . The fact that the function  $\Theta$  is not of positive type is no problem. Indeed, let its Fourier transform be written  $E(k) = E_1(k) - E_2(k)$ , where  $E(k) = E_1(k)$  whenever  $E(k) \geq 0$ . Using the step function amounts to replacing in (1) the real forcing  $f$  by the complex forcing  $f_1 + if_2$  where  $f_1$  and  $f_2$  are independent Gaussian random functions, white-noise in time and chosen such that their energy spectra (in the space variable) are respectively  $E_1(k)$  and  $E_2(k)$ . Since the passive scalar equation is linear, the solution may itself be written as  $\theta_1 + i\theta_2$  where  $\theta_1$  and  $\theta_2$  are the (independent) solutions of the passive scalar equations with respective forcing terms  $f_1$  and  $f_2$ . Using the universality with respect to the functional form of the forcing [25], it is then easily shown that the scaling laws for the passive scalar structure functions are the same as for real forcing.

We shall be interested in the passive scalar structure functions of even order  $2n$  (odd order ones vanish by symmetry), defined as

$$S_{2n}(r; L) \equiv \langle (\theta(\mathbf{r}) - \theta(\mathbf{0}))^{2n} \rangle. \quad (29)$$

From Ref. [6] (see also Ref. [15]) we know that, for  $L \gg r \gg \eta \sim \kappa^{1/\xi}$ , the second-order structure function is given by

$$S_2(r; L) = C_2 \varepsilon r^{\zeta_2}, \quad \zeta_2 = 2 - \xi, \quad (30)$$

where  $C_2$  is a dimensionless numerical constant. If there were no anomalies, we would have, for  $n > 1$ ,

$$S_{2n}(r; L) = C_{2n} \varepsilon^n r^{n\zeta_2}. \quad (31)$$

Note that (30) and (31) do not involve the integral scale  $L$ . Actually, for  $n > 1$ , we have *anomalous* scaling with  $S_{2n}(r; L) \propto r^{\zeta_{2n}}$  and  $\zeta_{2n} < n\zeta_2$ . More precisely, we have

$$S_{2n}(r; L) = C_{2n} \varepsilon^n r^{n\zeta_2} \left( \frac{L}{r} \right)^{\zeta_{2n}^{\text{anom}}}, \quad (32)$$

$$\zeta_{2n}^{\text{anom}} \equiv n\zeta_2 - \zeta_{2n}, \quad (33)$$

where the structure function now displays a dependence on the integral scale  $L$ . Our strategy will be to measure the dependence of  $S_{2n}(r; L)$  on  $L$  while the separation  $r$  and the injection rate  $\varepsilon$  are kept fixed and, thereby, to have a direct measurement of the anomaly  $\zeta_{2n}^{\text{anom}}$ .

Let us show that, in principle, this can be done by the Lagrangian method of Section II using  $2n$  tracer (Lagrangian) particles whose trajectories satisfy (15). The structure function of order  $2n$  can be written as a linear combination of moments of the form  $\langle \theta(\mathbf{r}_1) \theta(\mathbf{r}_2) \dots \theta(\mathbf{r}_{2n}) \rangle$ , where  $p$  of the points are at location  $\mathbf{r}$  and  $2n - p$  at location  $\mathbf{0}$  ( $p = 0, \dots, 2n$ ). Because of the symmetries of the problem,  $p$  and  $2n - p$  give the same contribution. Thus, we need to work only with the  $n + 1$  configurations corresponding to  $p = 0, \dots, n$ . For example, we have

$$S_4(r; L) = 2 \langle \theta^4(\mathbf{r}) \rangle - 8 \langle \theta^3(\mathbf{r}) \theta(\mathbf{0}) \rangle + 6 \langle \theta^2(\mathbf{r}) \theta^2(\mathbf{0}) \rangle. \quad (34)$$

Let us first consider the case of the two-point function (second-order moment). Using (14), (18) and the independence of  $\mathbf{v}$  and  $f$ , we have

$$\langle \theta(\mathbf{r}_1) \theta(\mathbf{r}_2) \rangle = \left\langle \int_{-T}^t \int_{-T}^t \langle f(\mathbf{a}_1(s_1), s_1) f(\mathbf{a}_2(s_2), s_2) \rangle_f ds_1 ds_2 \right\rangle_{vw}. \quad (35)$$

Here,  $\langle \cdot \rangle_f$  is an average over the forcing and  $\langle \cdot \rangle_{vw}$  denotes averaging over the velocity and the  $\dot{\mathbf{w}}$ 's, and  $\mathbf{a}_1(s_1)$  and  $\mathbf{a}_2(s_2)$  satisfy (15) with the “final” conditions  $\mathbf{a}_1(t) = \mathbf{r}_1$  and  $\mathbf{a}_2(t) = \mathbf{r}_2$ , respectively.

In (35) the averaging over  $f$  can be carried out explicitly using (28). With our step-function choice for  $F$ , we obtain

$$\langle \theta(\mathbf{r}_1) \theta(\mathbf{r}_2) \rangle = \langle T_{12}(L) \rangle_v, \quad (36)$$

where

$$T_{12}(L) = \int_{-T}^t \Theta_L(|\mathbf{a}_1(s) - \mathbf{a}_2(s)|) ds \quad (37)$$

is the amount of time that two tracer particles arriving at  $\mathbf{r}_1$  and  $\mathbf{r}_2$  and moving backwards in time spent with their mutual distance  $|\mathbf{a}_1(s) - \mathbf{a}_2(s)| < L$ . Whether the particles move backwards or forward in time is actually irrelevant for the Kraichnan model since the velocity, being Gaussian, is invariant under reversal.

For the four-point function, we proceed similarly and use the Wick rules to write fourth-order moments of  $f$  in terms of sums of products of second-order moments, obtaining

$$\begin{aligned} \langle \theta(\mathbf{r}_1) \theta(\mathbf{r}_2) \theta(\mathbf{r}_3) \theta(\mathbf{r}_4) \rangle &= \langle T_{12}(L) T_{34}(L) \rangle_{vw} \\ &+ \langle T_{13}(L) T_{24}(L) \rangle_{vw} \\ &+ \langle T_{14}(L) T_{23}(L) \rangle_{vw}. \end{aligned} \quad (38)$$

Expressions similar to Eqs. (36) and (38) are easily derived for higher order correlations.

We see that the evaluation of structure functions and moments has been reduced to studying certain statistical properties of the random time that pairs of particles spend with their mutual distances less than the integral scale  $L$ . Generally, the distance between pairs of particles tends to increase with the time elapsed but, occasionally, particles may come very close and stay so; this will be the source of the anomalies in the scaling.

## V. NUMERICAL IMPLEMENTATION OF THE LAGRANGIAN METHOD

In Section IV we have shown that structure functions of the passive scalar are expressible in terms of  $\mathbf{v}$ -averages of products of factors  $T_{ij}(L)$ . For the structure function of order  $2n$ , these products involve configurations of  $2n$  particles,  $p$  of which end at locations  $\mathbf{r}$  at time  $s = t$  and the remaining  $2n - p$  at location  $\mathbf{0}$ . In the Kraichnan model  $\mathbf{v}$  and  $f$  are stationary, so that after relaxation of transients,  $\theta$  also becomes stationary. We may thus calculate our structure functions at  $t = 0$ . Time-reversal invariance of the  $\mathbf{v}$  field and of the Lagrangian equations allows us to run the  $s$ -time forward rather than backward. Also,  $T_{ij}(L)$  is sensitive only to differences in particle separations, whose evolution depends only on the difference of the velocities at  $\mathbf{a}_i$  and  $\mathbf{a}_j$ . Furthermore, the  $\mathbf{v}$  field has homogeneous increments. All this allows us to work with  $2n - 1$  particle separations, namely

$$\tilde{\mathbf{a}}_i(s) \equiv \mathbf{a}_i(s) - \mathbf{a}_{2n}(s), \quad i = 1, \dots, 2n - 1, \quad (39)$$

$$\tilde{\mathbf{a}}_i(t) = \tilde{\mathbf{r}}_i \equiv \mathbf{r}_i - \mathbf{r}_{2n}. \quad (40)$$

Using (15) we find that the quantities  $\tilde{\mathbf{a}}_i(s)$  satisfy  $2n - 1$  (vector-valued) differential equations which involve the differences of velocities  $\mathbf{v}(\mathbf{a}_i(s), s) - \mathbf{v}(\mathbf{a}_{2n}(s), s)$ . The statistical properties of the solutions remain unchanged if we subtract  $\mathbf{a}_{2n}(s)$  from all the space arguments. We thus obtain the following Lagrangian equations of motion for the  $2n - 1$  particle separations:

$$\frac{d\tilde{\mathbf{a}}_i(s)}{ds} = \tilde{\mathbf{v}}_i(s) + \sqrt{2\kappa} \tilde{\mathbf{w}}_i(s) \quad (41)$$

$$\tilde{\mathbf{v}}_i(s) \equiv \mathbf{v}(\tilde{\mathbf{a}}_i(s), s) - \mathbf{v}(\mathbf{0}, s), \quad (42)$$

$$\tilde{\mathbf{w}}_i(s) \equiv \dot{\mathbf{w}}_i - \dot{\mathbf{w}}_{2n}. \quad (43)$$

For numerical purposes (41) is discretized in time using the standard Euler–Ito scheme of order one half [24]

$$\tilde{\mathbf{a}}_i(s + \Delta s) - \tilde{\mathbf{a}}_i(s) = \sqrt{\Delta s} (\mathcal{V}_i + \sqrt{2\kappa} \mathcal{W}_i), \quad (44)$$

where  $\Delta s$  is the time step and the  $\mathcal{V}_i$ 's and the  $\mathcal{W}_i$ 's ( $i = 1, \dots, 2n - 1$ ) are  $d$ -dimensional Gaussian random vectors chosen independently of each other and independently at each time step and having the appropriate correlations, which are calculated from (5) and (26), namely

$$\begin{aligned} \langle \mathcal{V}_{i,\alpha} \mathcal{V}_{j,\beta} \rangle &= \\ D_{\alpha\beta}(\tilde{\mathbf{a}}_i) + D_{\alpha\beta}(\tilde{\mathbf{a}}_j) - D_{\alpha\beta}(\tilde{\mathbf{a}}_i - \tilde{\mathbf{a}}_j), \end{aligned} \quad (45)$$

$$\langle \mathcal{W}_{i,\alpha} \mathcal{W}_{j,\beta} \rangle = (1 + \delta_{ij}) \delta_{\alpha\beta}, \quad (46)$$

where  $D_{\alpha\beta}(\mathbf{r})$  is defined in (27).

To actually generate these Gaussian random variables, we use the symmetry and positive definite character of covariance matrices like (45) and (46). Indeed, any such matrix can be factorized as a product (taking  $\mathcal{V}$  as an example) [26]

$$\langle \mathcal{V} \otimes \mathcal{V} \rangle = \mathcal{L} \mathcal{L}^T, \quad (47)$$

where  $\mathcal{L}$  is a nonsingular lower triangular matrix and  $\mathcal{L}^T$  is its transpose.  $\mathcal{L}$  can be computed explicitly using the Cholesky decomposition method [26], an efficient algorithm to compute the triangular factors of positive definite matrices. It nevertheless takes  $O([(2n - 1)d]^3/3)$  flops to get  $\mathcal{L}$  from  $\langle \mathcal{V} \otimes \mathcal{V} \rangle$  and this is the most time-consuming operation at each time step. Once  $\mathcal{L}$  is obtained, a suitable set of variables  $\mathcal{V}$  can be obtained by applying the linear transformation

$$\mathcal{V} = \mathcal{L} \mathcal{N} \quad (48)$$

to a set of *independent* unit-variance Gaussian random variables  $\mathcal{N}_{i,\alpha}$  coming from a standard Gaussian random number generator, that is with  $\langle \mathcal{N}_{i,\alpha} \mathcal{N}_{j,\beta} \rangle = \delta_{ij} \delta_{\alpha\beta}$ . The resulting variables  $(\mathcal{V}_i)_\alpha$  then have the required covariances.

From the  $\tilde{\mathbf{a}}_i(s)$ 's we obtain the quantities  $T_{ij}(L)$  for all the desired values of the integral scale  $L$ , typically, a

geometric progression up to the maximum value  $L_{\max}$ . The easiest way to evaluate  $S_{2n}(r; L)$  is to evolve simultaneously the  $n + 1$  configurations corresponding to  $p = 0, \dots, n$ , stopping the current realization when *all* inter-particle distances in *all* configurations are larger than some appropriate large-scale threshold  $L_{\text{th}}$ , to which we shall come back. The various moments appearing in the structure functions are then calculated using expression such as (38) in which the  $(v, w)$ -averaging is done by the Monte-Carlo method, that is over a suitably large number of realizations. We note that the expressions for the structure functions of order higher than two involve heavy cancellations between the terms corresponding to different configurations of particles. For instance, the three terms appearing in the expression (34) for the fourth-order function, all have dominant contributions scaling as  $L^{2(2-\xi)}$  for large  $L$  and a first subdominant correction scaling as  $L^{2-\xi}$ . The true non-trivial scaling  $\propto L^{\zeta_4^{\text{anom}}}$  emerges only after cancellation of the dominant and first subdominant contributions. For small  $\xi$  the dominant contributions are particularly large. In the presence of such cancellations, Monte-Carlo averaging is rather difficult since the relative errors on individual terms decrease only as the inverse square root of the number of realizations. In practice, the number of realizations is increased until clean non-spurious scaling emerges. In three dimensions, for  $S_4(r; L)$ , between one and several millions realizations (depending on the value of  $\xi$ ) are required. In two dimensions even more realizations are needed. For example, to achieve comparable quality of scaling for  $\xi = 0.75$ , in three dimensions  $4 \times 10^6$  realizations are needed but  $14 \times 10^6$  are needed in two dimensions.

Now, some comments on the choice of parameters.

The threshold  $L_{\text{th}}$  must be taken sufficiently large compared to largest integral scale of interest  $L_{\max}$  to ensure that the probability of returning within  $L_{\max}$  from  $L_{\text{th}}$  is negligible. But choosing an excessively large  $L_{\text{th}}$  is too demanding in computer resources. In practice, the choice of  $L_{\text{th}}$  depends both on the space dimension and on how far one is from the limit  $\xi = 0$ . In three dimensions, it is enough to take  $L_{\text{th}} = 10 L_{\max}$ . In two dimensions there is a new difficulty when  $\xi$  is small. At  $\xi = 0$  the motion of Lagrangian particles and also of separations of pairs of particles is exactly two-dimensional Brownian motion. As it is well-known, in two dimensions, Brownian motion is recurrent (see, e.g., Ref. [27]). Hence, with probability one a pair of particles will eventually achieve arbitrarily small separations. As a consequence, at  $\xi = 0$  in two dimensions, the mean square value of  $\theta$  is infinite. For very small positive  $\xi$  this mean square saturates but most of the contribution comes from scales much larger than the integral scale. This forces to choose extremely large values of  $L_{\text{th}}$  when  $\xi$  is small. In practice, for  $0.6 \leq \xi \leq 0.9$  we take  $L_{\text{th}} = 4 \times 10^3 L_{\max}$  and beyond  $\xi = 0.9$  we take  $L_{\text{th}} = 10 L_{\max}$ . (The range  $\xi < 0.6$  has not yet been explored.) In view of the accuracy of our results, we have verified that the use of larger values for  $L_{\text{th}}$  does

not affect in any significant way the values of the scaling exponents.

The molecular diffusivity  $\kappa$  is chosen in such a way that  $r$  is truly in the inertial range, namely, we demand (i) that the dissipation scale  $\eta \sim \kappa^{1/\xi}$  should be much smaller than the separation  $r$  and (ii) that the time a pair of particle spends with a separation comparable to  $\eta$ , which is  $\sim \eta^2/\kappa \sim \eta^{2-\xi}$  should be much smaller than the time needed for this separation to grow from  $r$  to  $L$ , which is  $\sim L^{2-\xi} - r^{2-\xi}$ . The latter condition becomes very stringent when  $\xi$  is close to 2.

Finally, the time step  $\Delta s$  is chosen small compared to the diffusion time  $\eta^2/\kappa$  at scale  $\eta$ .

## VI. RESULTS

We now present results for structure functions up to fourth order. The three-dimensional results have already been published in Ref. [10]. The two-dimensional results are new. Some results for structure functions of order six have been published in Ref. [28] and shall not be repeated here (more advanced simulations are in progress).

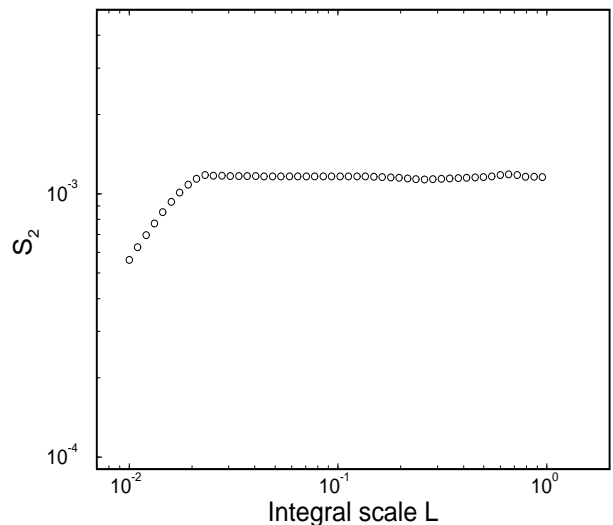


FIG. 1. 3-D second-order structure function  $S_2$  vs  $L$  for  $\xi = 0.6$ . Separation  $r = 2.7 \times 10^{-2}$ , diffusivity  $\kappa = 1.115 \times 10^{-2}$ , number of realizations  $4.5 \times 10^6$ .

A severe test for the Lagrangian method is provided by the second-order structure function  $S_2(r; L)$ , whose expression is known analytically [1]. Its behavior being non-anomalous, a flat scaling in  $L$  should be observed. The  $L$ -dependence of  $S_2$ , measured by the Lagrangian method, is shown in Fig. 1 for  $\xi = 0.6$  and  $d = 3$  (all structure functions are plotted in log-log coordinates). The measured slope is  $10^{-3}$  and the error on the constant is 3%. (These figures are typical also for other values of  $\xi$  studied.) We observe that, for separation  $r$  much larger than the integral scale  $L$ , correlations between  $\theta(\mathbf{r})$  and

$\theta(\mathbf{0})$  are very small; hence, the scaling for the second-order structure function is essentially given by the  $L$ -dependence of  $\langle \theta^2 \rangle$ , namely  $L^{2-\xi}$ ; the transition to the constant-in- $L$  behavior around  $r = L$  is very sharp, on account of the step function chosen for  $F$ .

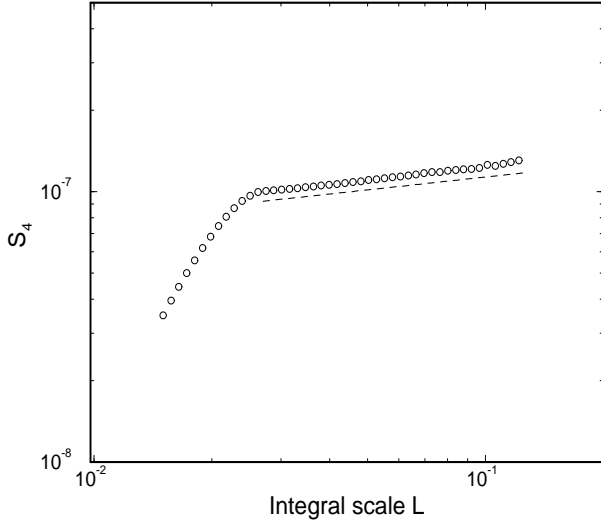


FIG. 2. 3-D fourth-order structure function  $S_4$  vs  $L$  for  $\xi = 0.2$ . Separation  $r = 2.7 \times 10^{-2}$ , diffusivity  $\kappa = 0.247$ , number of realizations  $15 \times 10^6$ .

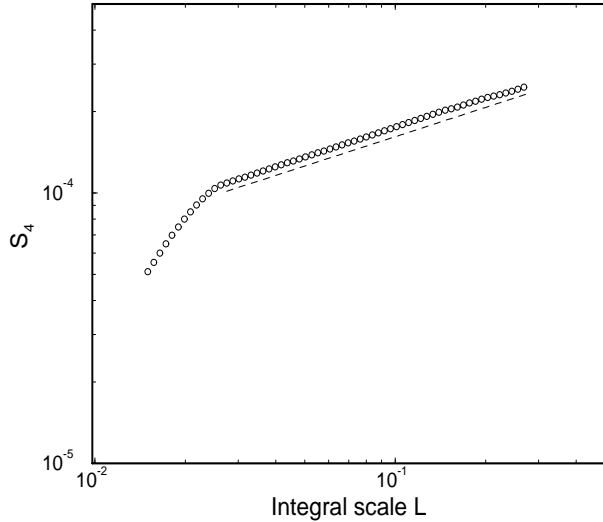


FIG. 3. Same as in Fig. 2 for  $\xi = 0.9$ . Parameters:  $r = 2.7 \times 10^{-2}$ ,  $\kappa = 4.4 \times 10^{-4}$ , number of realizations  $8 \times 10^6$ .

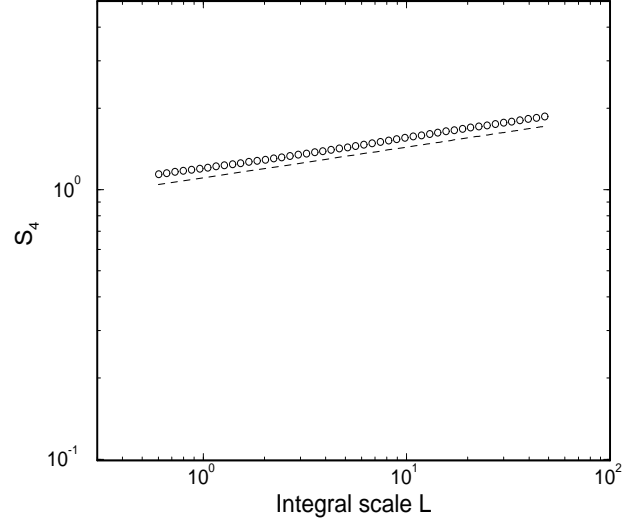


FIG. 4. Same as in Fig. 2 for  $\xi = 1.75$ . Parameters:  $r = 2.7 \times 10^{-2}$ ,  $\kappa = 10^{-9}$ , number of realizations  $1.5 \times 10^6$ .

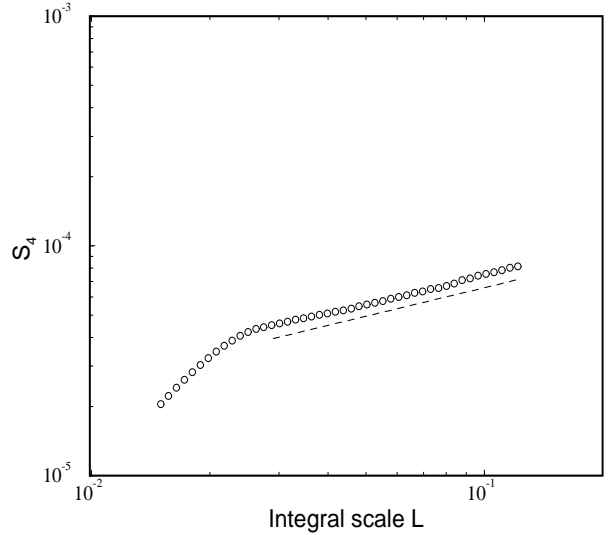


FIG. 5. 2-D fourth-order structure function  $S_4$  vs  $L$  for  $\xi = 0.6$ . Parameters:  $r = 2.7 \times 10^{-2}$ ,  $\kappa = 1.1 \times 10^{-2}$ , number of realizations  $5 \times 10^6$ .

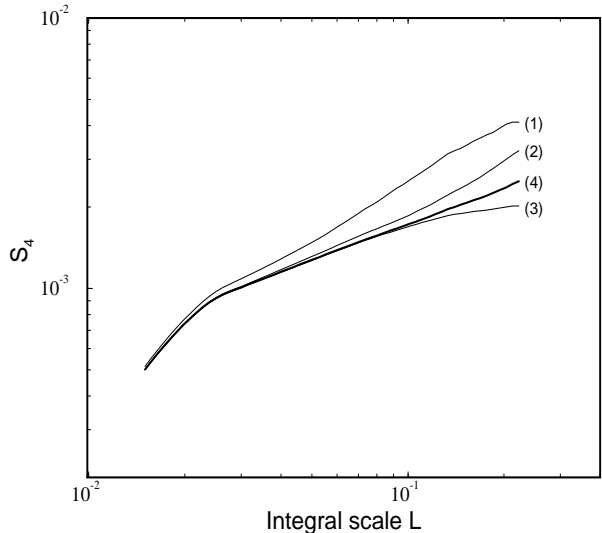


FIG. 6. Same as in Fig. 5 for  $\xi = 0.9$ . Parameters are  $r = 2.7 \times 10^{-2}$ ,  $\kappa = 4.4 \times 10^{-4}$ . To illustrate convergence, various numbers of realizations are shown: (1)  $150 \times 10^3$ , (2)  $1.5 \times 10^6$ , (3)  $3.4 \times 10^6$ , (4) from  $4.8 \times 10^6$  to  $7 \times 10^6$  (several curves superposed).

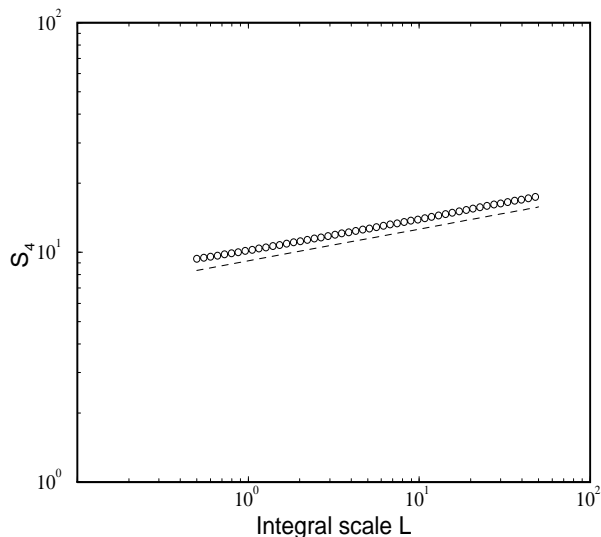


FIG. 7. Same as in Fig. 5 for  $\xi = 1.75$ . Parameters:  $r = 2.7 \times 10^{-2}$ ,  $\kappa = 10^{-9}$ , number of realizations  $2.4 \times 10^6$ .

Figs. 2, 3 and 4 show the  $L$ -dependence of the fourth-order structure function in three dimensions for  $\xi = 0.2$ , 0.9 and 1.75, respectively. In each case the scaling region (which is basically  $L > r$ ) is indicated by a dashed straight line whose slope is the anomaly. Note that, to obtain a similar high-quality scaling as shown on these figures, a much larger number of realizations is needed for small  $\xi$ ; this is required to permit cancellation of leading

contributions to (34), as explained in Section V.

The two-dimensional case, which is numerically more difficult for reasons explained near the end of Section V, is shown in Figs. 5, 6 and 7 for  $\xi = 0.6$ , 0.9 and 1.75, respectively. Fig. 6 also shows the data obtained for various values of the number of realizations. Note that if only  $150 \times 10^3$  realizations are used, the anomaly (that is the slope obtained, e.g., by a least square fit) is grossly overestimated.

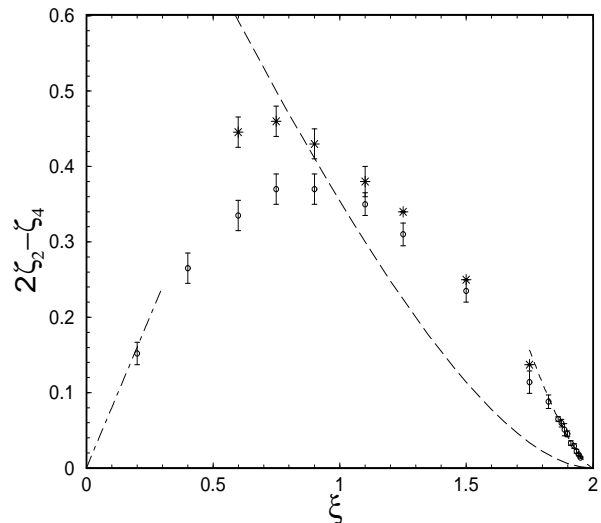


FIG. 8. The anomaly  $2\zeta_2 - \zeta_4$  for the fourth-order structure function in two dimensions (stars, upper graph) and three dimensions (circles, lower graph). Error bars in 2-D shown only for  $\xi \leq 1.1$ . The dashed line is the three-dimensional linear ansatz prediction (49).

Fig. 8 shows a plot of the anomaly  $\zeta_4^{\text{anom}}$  vs  $\xi$  in both two and three dimensions. The error bars (shown in 2-D only for  $\xi \leq 1.1$  to avoid crowding) are obtained by analyzing the fluctuations of local scaling exponents over octave ratios of values for  $L$ , a method which tends to overestimate errors.

Let us now comment on the results. In three dimensions, the error bars near  $\xi = 2$  are exceedingly small and the data have a good fit (shown as dashed line) of the form  $\zeta_4^{\text{anom}} = a\gamma + b\gamma^{3/2}$  with  $\gamma = 2 - \xi$  (the parameters are  $a = 0.06$  and  $b = 1.13$ ). This is compatible with an expansion in powers of  $\sqrt{\gamma}$  [29] in which a term  $\propto \sqrt{\gamma}$  is ruled out by the Hölder inequality  $\zeta_4 \leq 2\zeta_2 = 2\gamma$ .

Of particular significance is that, when  $\xi$  is decreased from 2 to 0, the anomaly grows at first, achieves a maximum and finally decreases. In three dimensions, where small- $\xi$  simulations are easier than in two dimensions, we have good evidence that the anomaly vanishes for  $\xi \rightarrow 0$  as predicted by the perturbation theory of Gawędzki and Kupiainen [2], whose leading order  $\zeta_4^{\text{anom}} = 4\xi/5$  is shown as a dot-dashed straight line on Fig. 8. Note that the next-order correction  $\propto \xi^2$  is known [30] but the conver-



gence properties of the  $\xi$ -series are not clear. The “linear ansatz” prediction for the anomaly given in Refs. [1,7], that is

$$\zeta_4^{\text{anom}} = \frac{3\zeta_2 + d}{2} - \frac{1}{2}\sqrt{8d\zeta_2 + (d - \zeta_2)^2}, \quad (49)$$

$$\zeta_2 = 2 - \xi, \quad (50)$$

is consistent with our results only near  $\xi = 1$ , the point farthest from the two limits  $\xi = 0$  and  $\xi = 2$ , which both have strongly nonlocal dynamics. This suggests a possible relation between deviations from the linear ansatz and locality of the interactions [31]. Whether this consistency for  $\xi = 1$  persists for moments of order higher than four is an open problem.

The fact that the anomalies are stronger in two than in three dimensions is consistent with their vanishing as  $d \rightarrow \infty$  [3]. The fact that the maximum anomaly occurs for a value of  $\xi$  smaller in two than in three dimensions can be tentatively interpreted as follows. Near  $\xi = 0$  the dynamics is dominated by the nearly ultraviolet-divergent eddy diffusion, whereas near  $\xi = 2$  it is dominated by the nearly infrared-divergent stretching. The former increases with  $d$ , but not the latter. The maximum is achieved when these two effects balance.

## VII. CONCLUDING REMARKS

Compared to Eulerian simulations of the partial differential equation (1) our Lagrangian method has various advantages. When calculating moments of order  $2n$  we do not require the complete velocity field at each time step but only  $2n - 1$  random vectors, basically, the set of velocity differences between the locations of Lagrangian tracer particles which are advected by the flow and subject to independent Brownian diffusion. As a consequence the complexity of the computation (measured in number of floating point operations) grows polynomially rather than exponentially with the dimension  $d$ . Furthermore, working with tracers naturally allows to measure the scaling of the structure functions  $S_{2n}(r; L)$  vs the integral scale  $L$  of the forcing. Physically, this means that the injection rate of passive scalar variance (which equals its dissipation rate) and the separation  $r$  are kept fixed while the integral scale  $L$  is varied. Anomalies, that is discrepancies from the scaling exponents which would be predicted by naïve dimensional analysis, are measured here directly through the scaling dependence on  $L$  of the structure functions.

Actually, direct Eulerian simulations and the Lagrangian method are complementary. Very high-resolution simulations of the sort found in Ref. [5] are really not practical in more than two dimensions but do give access to the entire Eulerian passive scalar field. Hence, they can and have been used to address questions about the geometry of the scalar field and about probability distributions.

Although we have presented here the numerical implementation of the Lagrangian method only for the Kraichnan model, it is clear that the general strategy presented in Sections II and III is applicable to a wide class of random flows, for example, with a finite correlation time.

An important aspect of the results obtained for the Kraichnan model is that they agree with perturbation theory [2] for  $\xi \rightarrow 0$ . As is now clear from theory and simulations, anomalies in the Kraichnan model and other passive scalar problems arise from zero modes in the operators governing the Eulerian dynamics of  $n$ -point correlation functions [2,3,32]. It is likely that some form of zero modes is also responsible for anomalous scaling in nonlinear turbulence problems. An instance are the “fluxless solutions” to Markovian closures based on the Navier–Stokes equations in dimension  $d$  close to two, which have a power-law spectrum with an exponent depending continuously on  $d$  [33]. Attempts to capture intermittency effects in three-dimensional turbulence are being made along similar lines (see, e.g., Ref. [34]). The Kraichnan model for passive scalar intermittency puts us on a trail to understanding anomalous scaling in turbulence.

## ACKNOWLEDGMENTS

We are most grateful to Robert Kraichnan for innumerable interactions on the subject of passive scalar intermittency over many years. We acknowledge useful discussions with M. Chertkov, G. Falkovich, O. Gat, K. Gawędzki, F. Massaioli, S.A. Orszag, I. Procaccia, A. Wirth, V. Yakhot and R. Zeitak. Simulations were performed in the framework of the SIVAM project of the Observatoire de la Côte d’Azur. Part of them were performed using the computing facilities of CASPUR at Rome University, which is gratefully acknowledged. Partial support from the Centre National de la Recherche Scientifique through a “Henri Poincaré” fellowship (AM) and from the Groupe de Recherche “Mécanique des Fluides Géophysiques et Astrophysiques” (MV) is also acknowledged.

- 
- [1] R.H. Kraichnan, “Anomalous scaling of a randomly advected passive scalar,” *Phys. Rev. Lett.* **72**, 1016 (1994).
  - [2] K. Gawędzki and A. Kupiainen, “Anomalous scaling of the passive scalar,” *Phys. Rev. Lett.* **75**, 3834 (1995).
  - [3] M. Chertkov, G. Falkovich, I. Kolokolov, and V. Lebedev, “Normal and anomalous scaling of the fourth-order correlation function of a randomly advected passive scalar,” *Phys. Rev. E* **2**, 4924 (1995).
  - [4] K. Gawędzki, “Intermittency of passive advection,” in *Advances in Turbulence VII*, edited by U. Frisch (Kluwer Academic Publishers, London, 1998).
  - [5] S. Chen and R.H. Kraichnan, “Simulations of a Randomly Advected Passive Scalar Field,” *Phys. Fluids* **10**,

- 2867 (1998).
- [6] R.H. Kraichnan, "Small-scale structure of a scalar field convected by turbulence," *Phys. Fluids* **11**, 945 (1968).
- [7] R.H. Kraichnan, V. Yakhot, and S. Chen, "Scaling relations for a randomly advected passive scalar," *Phys. Rev. Lett.* **75**, 240 (1995).
- [8] A.L. Fairhall, B. Galanti, V.S. L'vov, and I. Procaccia, "Direct numerical simulations of the Kraichnan model: scaling exponents and fusion rules," *Phys. Rev. Lett.* **79**, 4166 (1997).
- [9] U. Frisch and A. Wirth, "Inertial-diffusive range for a passive scalar advected by a white-in-time velocity field," *Europhys. Lett.* **35**, 683 (1996).
- [10] U. Frisch, A. Mazzino, and M. Vergassola, "Intermittency in passive scalar advection," *Phys. Rev. Lett.* **80**, 5532 (1998).
- [11] O. Gat, I. Procaccia, and R. Zeitak, "Anomalous scaling in passive scalar advection: Monte Carlo Lagrangian trajectories," *Phys. Rev. Lett.* **80**, 5536 (1998).
- [12] R.H. Kraichnan, "Lagrangian-history closure approximation for turbulence," *Phys. Fluids* **8**, 575 (1965).
- [13] U. Frisch, *Turbulence. The Legacy of A. N. Kolmogorov* (Cambridge Univ. Press, Cambridge, 1995).
- [14] A. Brissaud and U. Frisch, "Solving linear stochastic differential equations," *J. Math. Phys.* **15**, 524 (1974).
- [15] U. Frisch and A. Wirth, "Intermittency of passive scalars in delta-correlated flow: introduction to recent work," in *Proceedings of Turbulence Modeling and Vortex Dynamics*, (Istanbul, Turkey, 2–6 September, 1996). *Springer Lect. Notes Phys.* **491**, 53, edited by O. Boratav, A. Eden and A. Erzan (Springer, Berlin, 1997).
- [16] D. Bernard, K. Gawędzki, and A. Kupiainen, "Slow modes in passive advection," *J. Stat. Phys.* **90**, 519 (1998).
- [17] M. Chertkov, "Instanton for random advection," *Phys. Rev. E* **55**, 2722 (1997).
- [18] G.K. Batchelor, "Small scale variation of convected quantities like temperature in turbulent fluid," *J. Fluid Mech.* **5**, 113 (1959).
- [19] R.H. Kraichnan, "Convection of a passive scalar by a quasi-uniform random straining field," *J. Fluid Mech.* **64**, 737 (1974).
- [20] B.I. Shraiman and E.D. Siggia, "Lagrangian path integrals and fluctuations in random flow," *Phys. Rev. E* **49**, 2912 (1994).
- [21] M. Chertkov, G. Falkovich, I. Kolokolov, and V. Lebedev, "Statistics of a passive scalar advected by a large-scale two-dimensional velocity field: analytic solution," *Phys. Rev. E* **51**, 5609 (1995).
- [22] L.F. Richardson, *Collected Papers*, vol. 1, edited by P.G. Drazin, (Cambridge University Press, 1993).
- [23] E. Hopf, "Statistical hydrodynamics and functional calculus," *J. Ratl. Mech. Anal.* **1**, 87 (1952).
- [24] P.E. Kloeden and E. Platen, *Numerical Solution of Stochastic Differential Equations* (Springer, Berlin, 1992).
- [25] K. Gawędzki and A. Kupiainen, "Universality in Turbulence: an Exactly Soluble Model," in *Lecture Notes in Physics* **469**, 71, edited by H. Grosse and L. Pittner (Springer, Berlin, 1996).
- [26] A. Ralston and P. Rabinowitz, *A First Course in Numerical Analysis* (McGraw-Hill, New York, 1978).
- [27] W. Feller, *An Introduction to Probability Theory and its Applications*, Vol. 1, (J. Wiley & Sons, New York, 1950).
- [28] U. Frisch, A. Mazzino, and M. Vergassola, "Lagrangian dynamics and high-order moments intermittency in passive scalar advection," *Phys. Chem. Earth* (in press).
- [29] A. Pumir, B.I. Shraiman and E.D. Siggia, "Perturbation theory for the  $\delta$ -correlated model of passive scalar advection near the Batchelor limit," *Phys. Rev. E* **55**, R1263, (1997).
- [30] L.T. Adzhemyan, N.V. Antonov, and A.N. Vasil'ev, "Renormalization group, operator product expansion, and anomalous scaling in a model of advected passive scalar," *Phys. Rev. E* **58**, 1823 (1998).
- [31] R.H. Kraichnan, private communication (1998).
- [32] B.I. Shraiman and E.D. Siggia, "Anomalous scaling of a passive scalar in turbulent flow," *C. R. Acad. Sci. Paris, série II* **321**, 279 (1995).
- [33] U. Frisch, M. Lesieur, and P.-L. Sulem, "On crossover dimensions for fully developed turbulence," *Phys. Rev. Lett.* **37**, 895 (1976); U. Frisch and J.-D. Fournier, "d-dimensional turbulence," *Phys. Rev. A* **17**, 747 (1978).
- [34] V.I. Belinicher, V.S. L'vov, A. Pomyalov, and I. Procaccia, "Computing the scaling exponents in fluid turbulence from first principles: demonstration of multiscaling," *J. Stat. Phys.* **93**, 797 (1998). (see also chao-dyn/9708004.)

FIGURE CAPTIONS

Fig. 1. 3-D second-order structure function  $S_2$  vs  $L$  for  $\xi = 0.6$ . Separation  $r = 2.7 \times 10^{-2}$ , diffusivity  $\kappa = 1.115 \times 10^{-2}$ , number of realizations  $4.5 \times 10^6$ .

Fig. 2. 3-D fourth-order structure function  $S_4$  vs  $L$  for  $\xi = 0.2$ . Separation  $r = 2.7 \times 10^{-2}$ , diffusivity  $\kappa = 0.247$ , number of realizations  $15 \times 10^6$ .

Fig. 3 Same as in Fig. 2 for  $\xi = 0.9$ . Parameters:  $r = 2.7 \times 10^{-2}$ ,  $\kappa = 4.4 \times 10^{-4}$ , number of realizations  $8 \times 10^6$ .

Fig. 4. Same as in Fig. 2 for  $\xi = 1.75$ . Parameters:  $r = 2.7 \times 10^{-2}$ ,  $\kappa = 10^{-9}$ , number of realizations  $1.5 \times 10^6$ .

Fig. 5. 2-D fourth-order structure function  $S_4$  vs  $L$  for  $\xi = 0.6$ . Parameters:  $r = 2.7 \times 10^{-2}$ ,  $\kappa = 1.1 \times 10^{-2}$ , number of realizations  $5 \times 10^6$ .

Fig. 6. Same as in Fig. 5 for  $\xi = 0.9$ . Parameters are  $r = 2.7 \times 10^{-2}$ ,  $\kappa = 4.4 \times 10^{-4}$ . To illustrate convergence, various numbers of realizations are shown: (1)  $150 \times 10^3$ , (2)  $1.5 \times 10^6$ , (3)  $3.4 \times 10^6$ , (4) from  $4.8 \times 10^6$  to  $7 \times 10^6$  (several curves superposed).

Fig. 7. Same as in Fig. 5 for  $\xi = 1.75$ . Parameters:  $r = 2.7 \times 10^{-2}$ ,  $\kappa = 10^{-9}$ , number of realizations  $2.4 \times 10^6$ .

Fig. 8. The anomaly  $2\zeta_2 - \zeta_4$  for the fourth-order structure function in two dimensions (stars, upper graph) and three dimensions (circles, lower graph). Error bars in 2-D shown only for  $\xi \leq 1.1$ . The dashed line is the three-dimensional linear ansatz prediction (49).